Investigation on three-dimensional marine dune modelling validation

Nicolas Michelet[1], Fabien Leckler[1], Maelle Nexer[1], Noémie Durand[1] and Alice Lefebvre[2]

[1]France Energies Marines, 525 Avenue Alexis de Rochon, 29280 Plouzané, France.

[2]Marum – Center for Marine environment Sciences, University of Bremen, Germany.

Corresponding author: Nicolas Michelet (nicolas.michelet@france-energies-marines.org)

Key Points:

- Marine dune
- Morphodynamic model
- Validation method

Abstract

The comparison of a morphodynamic model results with observations is an essential part to establish its credibility. In the past multiple models were validated against observations for sand banks, coastlines or estuarine environments. Some models have studied the marine dunes migrations but are generally limited to a two-dimensional study. In the present study, a three-dimensional morphodynamic model was setup on an area where highly dynamic dunes are present. The modelling results were analysed and compared to *in-situ* observations either using a 2D or a 3D method. The vertical and horizontal differences with observations were then assessed using the known method and, based on these results, an updated validation method were proposed to overcome some issues that could interfere with the process.

Plain Language Summary

To assess the reliability of a model, an essential part is to compare the results with field measurements. In the past, multiple models were setup up on sand banks, coastlines or estuarine environments and takes credibility with this kind of comparisons. Studies of the marine dune migration is generally made along two dimensions: the migration direction and the water depth. In the present study, a model is setup on a marine environment and accounts for three-dimensions to analyze the dunes' evolution over an area. The model validity is assessed using the known method and based on these results, an updated validation method was proposed to overcome some issues that could interfere with the process.

1 Introduction

The development of marine renewable energy has become a priority for many countries as part of the solution to limit the impacts of climate change while considering the global growing need in electricity. In the European Union, the offshore wind industry aims for an installed capacity of 300 GW by 2050. This will surely induce the multiplication of infractructures in the North Sea and the English Channel as it accounts for a large part of the energy potential. These shallow seas are however covered by active bedforms (Le Bot & Trentesaux, 2004 ; Damen et al., 2018) with heights that can reach 20-25 % of the water depth (Knaapen et al., 2001; Damen et al., 2018) and migration speeds up to tens of meters per year (Blondeaux and Vittori, 2016). Given these characteristics, these bedforms, also called marine dunes, are likely to pose specific challenges for the offshore windfarm industry. Their migration could induce scouring issues around the foundations or expose the burried cables over time increasing the risk of damage (Whitehouse et al., 2000 ; Barrie and Conway, 2014).

To understand the impact of marines dunes on offshore structures and vice versa, numerical modelling appears as one solution. Multiple numerical process-based models were developed to investigate marine dune migration, height and shape evolution over time and the processes that affect them (Németh et al., 2007 ; Van den Berg et al., 2012 ; Doré et al., 2018). However, most of these studies are focused on dune development starting from a flat bed which limits their applicability to study the long term evolution of marine dune fields. Tonnon et al. (2007) and Krabbendam et al. (2021) were the first to model dune dynamics over multiple years starting with an initial realistic bathymetry. They assessed the capability of the model to reproduce the evolution of large bedforms over a decade. For this, they used a two-dimensional vertical (2DV)

numerical model. The results were compared to the evolution of a dune field along a bathymetric transect extracted perpendicular to the crestlines. In areas where dunes are mostly rectilinear, it is reasonable to assume that most variations will be captured by a transect. However, most marine dune fields exhibit at least some degree of three-dimensionnality which would not be well represented using a 2D model. The use of a three-dimensional (3D) model seems thus necessary. However, how a morphodynamic model can be validated specifically to assess its ability to reproduce marine dune evolution is not yet established.

To validate a morphodynamic model over a shallow water area, the Brier Skill Score (BSS) is often used (Sutherland et al., 2004, Luijendijk et al., 2017). This single-number metric allows to assess the relative accuracy of morphodynamic simulations based on height difference between final observed and modelled states weighted with an initial state (Sutherland et al., 2004). This skill score has been used for modelling of coastlines (Luijendijk et al., 2017 ; Bennet et al., 2019), sand banks and bar movement (Sutherland et al., 2004) or even estuarine evolution (Scott and Mason, 2007 ; Dam et al., 2016). However, these studies mainly focus on coastal areas where the water depth is the key variable to assess the reliability of the models. For bedforms migrations, the water depth is also an important aspect but the use of only the BSS on the water depth might not be sufficient for the validation process. For example, Sutherland et al. (2007) have described a sand bar migration to illustrate the application of the BSS. The modelling of the outer bar depth shows a good agreement, while a significant error is estimated on the crest position. In their study it represents only one crest and does not impact the results. However, on other areas, differences on the crest positions could induce a misrepresentation of the sediment flux and bring errors on the long-term simulation. The crest positions might then need to be considered in the validation process.

The present study addresses the question of the validation of a morphodynamic model focused on the estimation of marine dune migration. The study area, off the Dunkirk coast, is described in section 2.1. The numerical systems, the Coastal and Regional Ocean COmmunity (CROCO) (Auclair et al., 2022) coupled with the USGS sediment module (Blaas et al., 2007 ; Warner et al., 2008) and their setup, in the eastern part of the English Channel and the southern part of the North Sea, are described in section 2.2 and section 2.3. The validation of the hydrodynamic predictions were assessed against in-situ measurements (section 3.1). Morphodynamic results, were studied either following a two-dimensional (section 3.2) and a three-dimensional (3D) (section 3.3) method before the proposal of a 3D validation of the modelling of the migration of marine dunes (section 3.4). All results are finally discussed in section 4.

2 Data and method

2.1 Study site

The site of application is located off the Dunkirk coasts in the southern part of the North Sea, a few kilometers east of the Dover Strait (Figure 1, left) in France. In this area the hydrodynamics are dominated by the tidal currents with a typical mean spring tidal range of 5.5 m at the Dunkirk tide gauge.

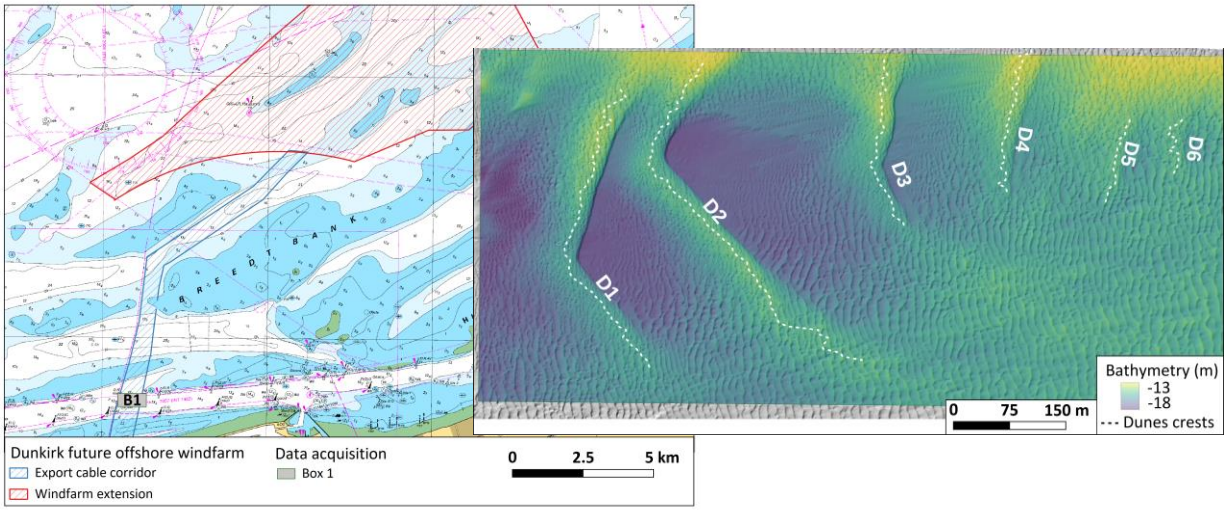

Figure 1. (left) Location of Dunkirk windfarm area (in red) and the area of interest where bathymetric surveys were performed noted B1 on the figure. (right) Bathymetric data of B1 area collected on the first survey of the 17 November 2019. All six dunes are numbered on the figure (D1-D6) and their crestlines are represented by the white dash-lines.

In this area, the tidal wave is considered progressive (Bonnefille et al., 1971). As a result, the maximum flood and ebb current magnitude happen at the time of, respectively, the high and low water level. The flood component, trending north-east with current amplitude up to 1.25 m/s, is generally stronger than the ebb which is directed toward the south-west with current amplitude up to 0.75 m/s (Figure 2, left). Regarding the waves, a major direction of origins was identified with the measurements of the Westhinder lightboat. Waves principally comes from the English Channel in the south-west while the rest comes from the inner basin of the North Sea in the north-west and north-east. Still according to the measurements, waves height range from 1 to 3 m and their periods are between 4 and 10 s (Figure 2, right).

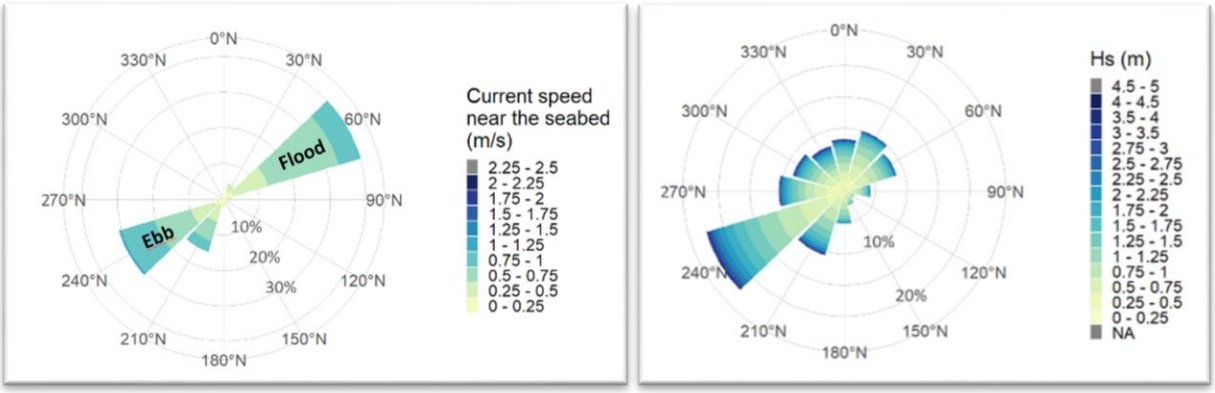

Figure 2. (left) Current speed near the seabed rose based on ADCP measurement (Nexer et al., 2023). (right) Offshore wave rose at Westhinder lightboat (51°22'51" N – 2°26'08" E) (Source data: Flanders Marine Institute).

This study focuses on a domain referred to as B1 (Figure 1, right), located along the future windfarm export cable corridor (Figure 1, left). Over this B1 area, 8 bathymetric surveys and multiple sediment samplings were performed between November 2019 and July 2021. In this study the bathymetry is expressed as the water depth with respect to the mean sea level (MSL). With a bathymetry ranging from 15 to 20 m, the area is composed of six very large dunes named D1-D6 with, from west to east, two barchans, a sinuous and three rectilinear dunes (Figure 1, right). The bathymetric data were analyzed in a preliminary study where a low-pass filter was applied to remove most secondary bedforms. The filtering is intentionally kept light to avoid too much modification of the primary dunes. Crests and troughs were identified manually respectively as the lowest and highest bathymetry point along longitudinal profiles (Nexer et al., 2023). According to these results, dune height and crestline length are decreasing from west to east (Table 1). The two barchans D1 and D2 are the largest dunes with respectively average height of 2.12 and 2.03 m and crestline length of 509.8 m and 599.52 m. Except for dune D4, the width (distance between the two dune troughs), follow the same schema with a value decreasing from west to east. The presence of the two barchans suggests that there is either a strong lateral variability of the sediment type (Ernsten et al., 2004) or a lack of sediment (Belderson et al., 1982). Bed samples showed that the seabed is uniformly composed of medium sand with d_{50} = 327.78 µm and d90 = 557.62 µm. Therefore, there is some indication that the environment may be sediment-starved.

Table 1. Heights, lengths and crestline lengths of all six dunes of B1 area measured on November the 17th 2019 (Nexer et al., 2023).

Dune name	Dune 1	Dune 2	Dune 3	Dune 4	Dune 5	Dune 6
Height (m)	2.12	2.03	1.64	1.16	0.92	0.78
Width (m)	140	140	135	152	132	66
Crestline length (m)	510	600	290	230	124	100

The comparison between the different surveys shows that the area is highly dynamic with a migration directed to the east at an average rate of 28.5 m/year with high variations between the different periods (Nexer et al., 2023). This eastern migration is explained by the influence of the asymmetrical tidal flow (Nexer et al., 2023). In this study, the 4 months period between the first 2 surveys (S1 on 17 November 2019 and S2 on 18 March 2020) are considered. During this period the dunes were highly dynamic with a migration rate ranging from 53.4 to 64.4 m/year. Figure 3 represents the bathymetric difference between these observations. Over the locations of each dune, eastward migration can be recognised as a positive difference on the western part of each dunes and a negative difference on the eastern part. Height differences up to 2.5 m are observed around the middle of the first two dunes while these changes decrease to 1.8 m on the northern part of Dune 3 and around 1 m for the other three dunes. These results imply that during these 4 months, the crests have moved toward the east and are standing on the initial eastern troughs positions. During the study period, the general migration schema can then be summarized as a movement of each dunes through the east with no significant changes of their horizontal shapes.

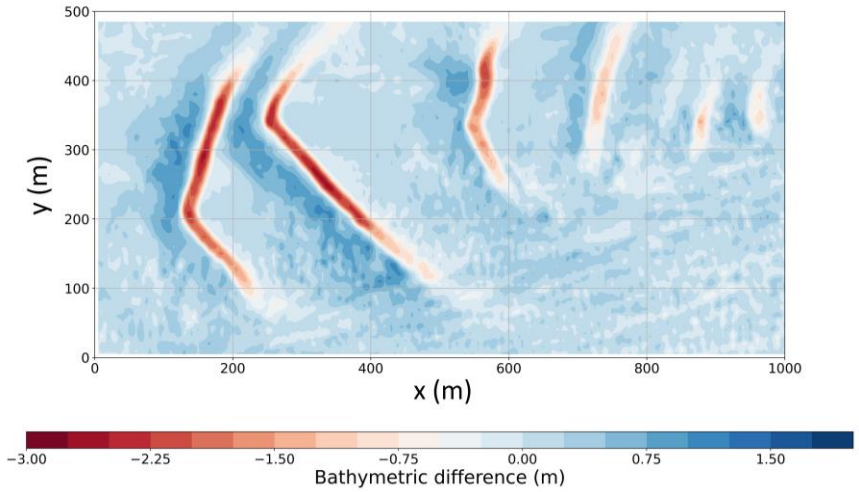

Figure 3. Bathymetric difference between final (S2) (18/03/2020) and initial (S1) (17/11/2019) observations.

2.2 Models description

CROCO is a three-dimensional, free-surface numerical model that solves finite-difference approximation of the Reynolds-Averaged Navier Stokes (RANS) equation using the hydrostatic and Boussinesq approximations. The computation is performed using a C-Arakawa grid over horizontal dimensions and a terrain-following σ coordinate along the vertical dimension. The set of equations is finally resolved using the mode-splitting technique that separates the barotropic and baroclinic modes.

The morphodynamic is modelled using the USGS sediment model. The sediment is represented as a constant number of layers that extend under the horizontal water cells (Warner et al., 2008). Each layer is initialized with a thickness, sediment-class distribution, porosity and age. To account for erosion and deposition, the active bed layer thickness evolves in time depending on the transport. Here only the bedload transport is considered following the Wu & Lin (2014) formulation which calculate the net transport rate as the sum of offshore and onshore bed-load transport rate. The bed evolution is calculated using the Exner equation considering only bedload transport.

2.3. Hydrodynamic setup

The computational domain has a 5 m horizontal resolution and covers the entire B1 area. The flow is assumed to be turbulent over a rough bottom, characterized by the roughness parameter z_0 defined as the height above the seabed at which the fluid velocity is zero. This parameter is defined as constant over the area of modelling. It was set to 0.4 and 4 mm in the two configurations considered in this study, referred to as C1 and C2. The calculation was performed with a baroclinic timestep of Δt_{3d} = 1 s and a barotropic timestep of Δt_{2D} = 1/12 s. Initial bathymetry is based on the initial survey performed on 17 November 2019 that were filtered as described before. C1 and C2 configurations have been performed using boundary conditions extracted from results coming from regional simulations using CROCO and WAVEWATCHIII® (WW3) models. Both were setup to downscale from a large-scale domain to the same grid,

named LS2, that cover the future windfarm area of Dunkirk and the cable corridor with a spatial resolution of 100 m (Figure 4).

CROCO

CROCO model downscale from a numerical domain that covers the eastern part of the English Channel and the southern part of the North Sea, called LS1 to LS2 domains (Figure 4). For both configurations, wind conditions were set using the AROME database. Boundary conditions of free-surface elevation and meridional and zonal component of the current were extracted from the MARC database (MARS3D configurations covering the French coasts and run operationally by Ifremer). The LS2 configuration considers LS1 results as boundaries. Along the water column, CROCO grid is configured using a total of 32 layers.

WAVEWATCHIII®

The wave model WAVEWATCHIII® (WW3) is based on nested runs that are implemented to downscale from global scale to fine resolution grids. First, the global-scale simulation is obtained using a regular computational grid with a 0.5-degree spatial resolution forced with ERA5 wind fields. Then, an unstructured mesh, called NORGAS developed by Shom and run operationally for the French marine surge monitoring is used. NORGAS's mesh refines from 10 km resolution at the open deep-water boundaries to 250 m resolution at the coast. The mesh covers the Gulf of Biscay, the English Channel and the south of the North Sea and benefits from an accurate bathymetry. The wave model is forced with currents and water levels obtained from the 2 km-resolution ATLNE model of the MARC database. Wind forcing using ERA5 hindcast is consistently used. On the computational grid LS2, the model is forced at the open boundaries with the wave spectra obtained with the NORGAS mesh and current and water levels from CROCO regional run LS1. Consistently with ocean model, the high-resolution wave model grid is forced with AROME database.

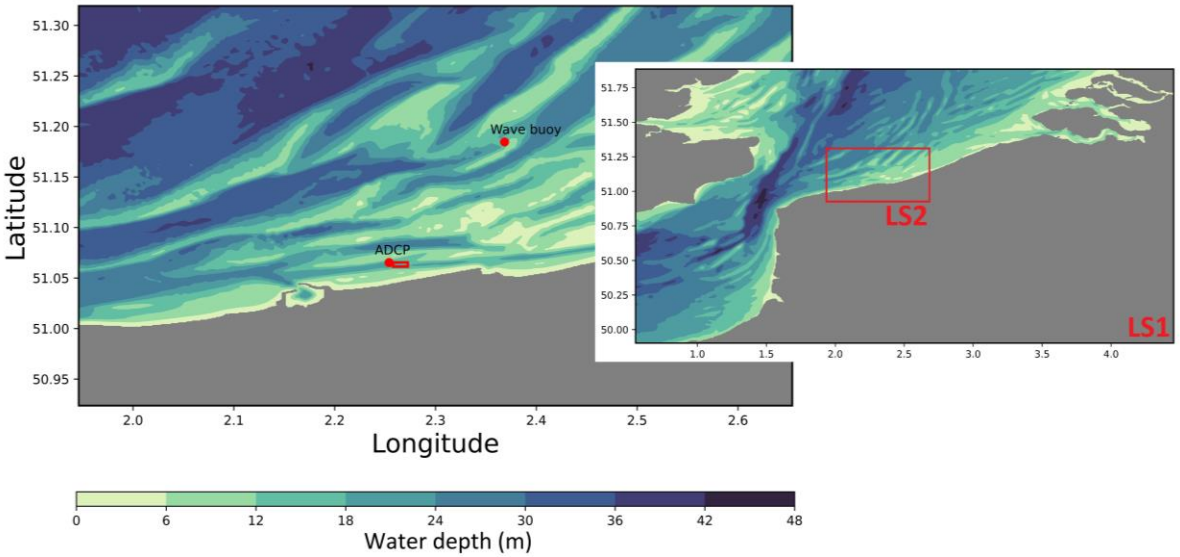

Figure 4. (left) Boundaries of the regional domain LS2. The locations of the ADCP and the wave buoy used for hydrodynamic validation are defined by the red dots. Area B1 is represented by the red box. (right) Boundaries of the regional domain LS1. The red box

represents the extension of the LS2 domain. Both color scales show the spatial distribution of the mean water depth, with respect to the mean sea level.

2.3. Morphodynamic setup

In-situ analysis showed that the sediment is homogeneous over the area. Hence, a class of medium sand with d_{50} = 328 µm is considered in the distribution. As reported before, the presence of barchans suggest that this area is sediment-starved. Since sampling performed either on the crests and troughs shows similar type of sediment (Nexer et al., 2023), considering the size of the dunes, a 3-m thick active layer is defined in this configuration which leaves enough amplitude to model the observed bathymetric differences (Figure 3). The porosity is set constant to 0.41 based on the analysis of the in-situ samples. Since no suspended sediment is considered, the sediment age is left to 0 the default value.

2.4. Outputs analysis

Hydrodynamic and morphodynamic results were assessed using the Root Mean Square Error (RMSE):

$$RMSE = \sqrt{\frac{\sum_{i=1}^{N}\left(X_{mod,i} - X_{obs,i}\right)^2}{N}}$$

where X_{mod} and X_{obs} are respectively the predicted and observed variable and N the number of compared values. The hydrodynamic results were also evaluated using the index of agreement described by Willmott (1981) as:

$$RE = 1 - \frac{\sum_{i=1}^{N}\left(X_{obs,i} - X_{mod,i}\right)^2}{\sum_{i=1}^{N}\left(\left|X_{mod,i} - \overline{X_{obs}}\right| + \left|X_{obs,i} - \overline{X_{obs}}\right|\right)^2}$$

where the overbar $\overline{X_{obs}}$ is the averaged of the observation. The index of agreement ranges from 0 to 1 which described a perfect modelling.

The wave model performance was evaluated by comparing the significant wave height, mean direction and mean wave period T_{01}. The comparison is focused on T_{01} for its low order which gives more weight to the energetic waves, which are more important for sediment transport, than another type of period.

The morphodynamic analysis was based on the Brier Skill Score (BSS) (Sutherland et al., 2004) which is described as follow:

$$BSS = 1 - \frac{\langle (z_{mod} - z_{obs})^2 \rangle}{\langle (z_{ini} - z_{obs})^2 \rangle}$$

where z_{ini} is the initial bed level (here survey made the 17 November 2019), z_{obs} the final observation (here survey made the 18 March 2020) and z_{mod} the modelled bed level which is extracted on the same date as the final observation. The angular brackets $\langle \cdot \rangle$ denote the mean

over the area of interest. The BSS was also decomposed following the Murphy-Epstein decomposition (Murphy and Epstein, 1989) as follow:

$$BSS = \frac{\alpha - \beta - \gamma + \varepsilon}{1 + \varepsilon}$$

where α is the phase error which described the error in position. Perfect modelling of the phase gives α=1. β is the amplitude error which described the error in terms of sediment volume displacement with perfect modelling with β=0. γ is the averaged bed level error with perfect modelling with γ=0. And to finish the ε represent the normalization term which is only affected by the measured changes from the baseline prediction (Sutherland et al., 2004).

$$\alpha = r^2_{\Delta_{mod},\Delta_{obs}} \qquad \beta = \left(r_{\Delta_{mod},\Delta_{obs}} - \frac{\sigma_{\Delta_{mod}}}{\sigma_{\Delta_{obs}}} \right)^2$$

$$\gamma = \left(\frac{\langle \Delta_{mod} \rangle - \langle \Delta_{obs} \rangle}{\sigma_{\Delta_{obs}}} \right)^2 \qquad \varepsilon = \left(\frac{\langle \Delta_{obs} \rangle}{\sigma_{\Delta_{obs}}} \right)^2$$

with $r_{\Delta_{mod},\Delta_{obs}} = \frac{\langle \Delta_{mod}\Delta_{obs} \rangle}{\sigma_{\Delta_{mod}}\sigma_{\Delta_{obs}}}$, $\Delta_{mod} = z_{mod} - z_{ini}$ and $\Delta_{obs} = z_{obs} - z_{ini}$.

3 Results

3.1 Hydrodynamic validation

The first step is the hydrodynamic validation. Since no measurements were performed on the study area, the model was validated against Acoustic Doppler Current Profiler (ADCP) and wave buoy using the LS2 configurations of CROCO and WW3. Sensitivity analysis was performed on the hydrodynamic changes occuring between LS2 and B1 area modelling (B1 boundary conditions are extracted from LS2) to find that no significant changes occurred and the validation at LS2 level is considered valid at B1 level.

The comparison of the simulated and measured currents was performed over its barotropic component. Figure 5 shows the comparison of the current magnitude and direction between 20 May 2021 and 04 June 2021. The asymmetry between ebb and flood is well represented for the weak tidal conditions around 03 June while for the intense conditions in the middle of the comparison period, the model underestimates the flood peak. This could be attributed to the difference of bathymetry since LS2 configuration consider the HOMONIM bathymetry which has been surveyed in 2012. This difference stays however low with a RMSE = 0.16 m/s. Regarding the direction, the variation between ebb and flood is well represented with the direction varying between 75 and 265°N. The rapid turning of the tide at the beginning of each ebb/flood period is correctly represented despite some misrepresentation of short-term variations that sometimes occurs. It naturally increases the RMSE = 59.07° but the Willmott (1981) index shows that the representation stays correct with a value of 0.9.

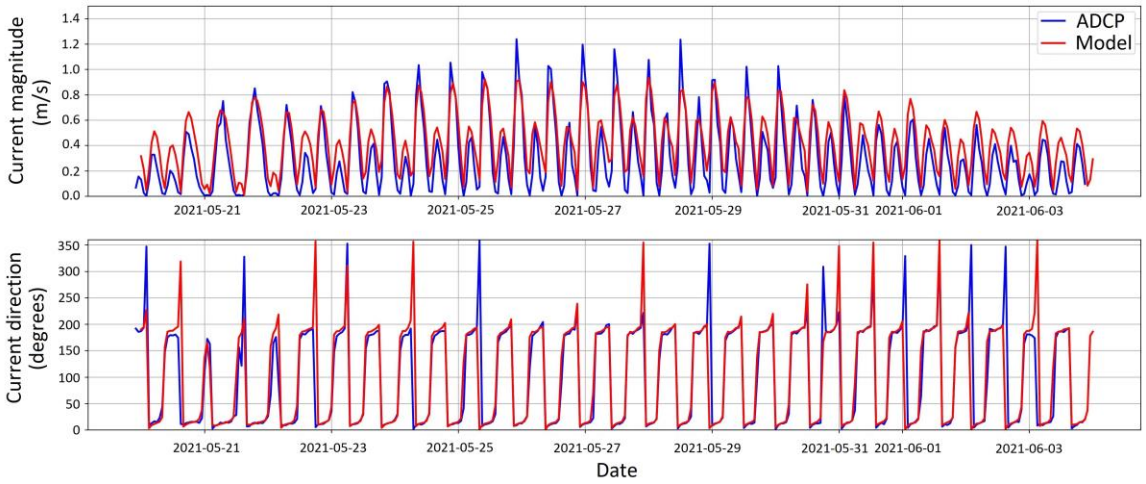

Figure 5. Current magnitude and direction comparison between model and ADCP measurements.

Regarding the waves, the following Figure 6 represents the comparison between model and observations between the 21 and the 30 May 2021. It shows an overall good accuracy of all components with correct statistics. The model accurately represents the variation of the significant wave height (RMSE = 0.16 m) which rises at the beginning of the period to reach almost 2.5 m on the first day and rapidly decreases to stay around 1 m for the following days. The wave period here does not show strong gradients and the model is in accordance with that with correct RMSE = 0.47. The RMSE value is however a boosted here by the fact that both model and buoy data do not actually show the same thing. The model returns current-corrected wave period, which is called the relative period, while we can see a clear variation due to the tidal current on the buoy data which returns the absolute wave period. This influence and the general discrepancy between model and measurements is however weak and the model is considered valid. To finish, the wave direction shows a very good match with even the rapid variations occurring on 26 May when the direction value drops from 315°N to 260°N within a couple of hours. Both RMSE = 18° and Willmott index of 0.96 demonstrates the good correlation of the model.

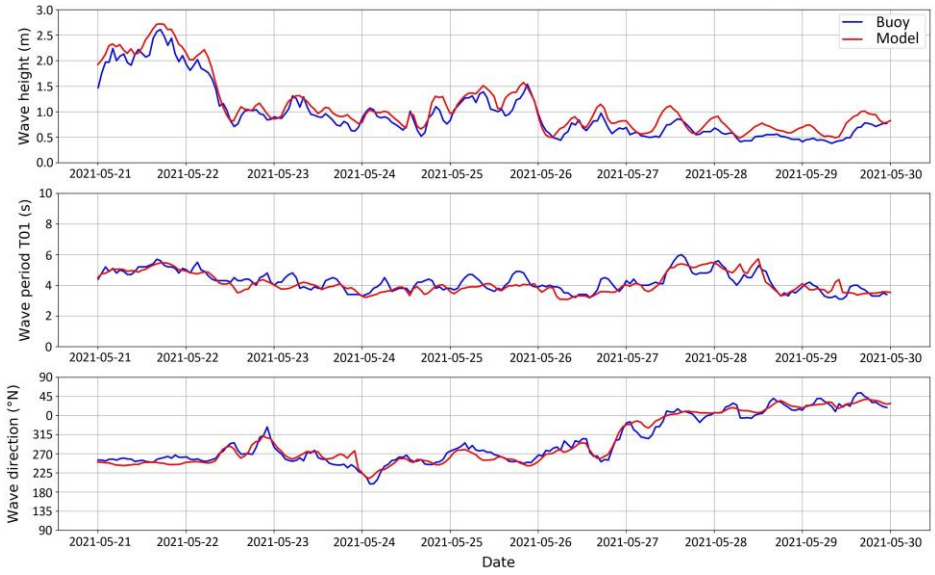

Figure 6. Significant wave height, T01 period and mean wave direction comparison between WW3 simulation and the wave buoy.

3.2 Comparison with observations along transects

A first analysis of the morphodynamic results was carried out along a transect extracted following a line perpendicular to the crestlines. However, since two barchans and a sinuous dune are present in the domain, several lines perpendicular to the crestlines can be defined. Therefore, the transect was extracted along the perpendicular of the three rectilinear dunes to catch all six dunes in a single row. On Figure 7, the longitudinal profile of the initial (S1) and final (S2) observations are compared to the modelling results of both C1 and C2 configurations. Observed data were submitted to the same low-pass filter to remove the secondary bedforms present throughout the study area. However, this filter is intentionnaly kept light and some secondary bedforms remain. To remove most of these small bedforms without changing the shape of the dune, the bathymetry is then smoothed a second time by applying a focal average. It considers a circle of 9 cells diameter (45 m considering the grid resolution) that slides along the domain and averages the center value by considering its neighbors. The observations are finally interpolated on the 5-m resolution modelling grid results to stay consistent with the model. Following the methodology of Nexer et al. (2023), the crests of all dunes are defined as the local minimum of water depth.

On this transect, difference between S1 and S2 shows that the crest height of the first three dunes (D1, D2 and D3) decrease in height by about 0.3 m. Furthermore, the vertical shape of the third dune is also modified with a rounder crest during the second survey than during the first. The three rectilinear dunes (D4, D5 and D6) do not show major changes in their crest height. They follow the general migration schema and migrate toward the east without significant changes. The model results generally follow the migration tendency revealed by the bathymetric surveys. The major difference between C1 and C2 configurations is the dune migration: migration rate is higher in C2 case and better matches the observation especially for the three rectilinear dunes than for C1. This result is in accordance with the roughness parameters which is 10 times higher for C2 than for C1. Regarding the crest height, both configurations show a similar pattern. Contrary to the observed morphodynamic, the model estimates an increase in the crest height of

D1 but underestimate it for D2 (difference of almost 0.7 m with S1 compared to a reduction of 0.3 m in reality). The model accurately represents the variation of D3 and is consistent for both C1 and C2. For all dunes, C2 configuration is closer than C1 to the measured bathymetry with a better representation of the migration rate. This is confirmed by the Brier Skill Score (BSS_{C1} = 0.75 and BSS_{C2} = 0.87). Following the classification proposed by Sutherland et al. (2004), both configurations can be considered as excellent. The model aims at correctly simulating dune dynamics, therefore the crest positions are important to consider the modelling as accurate. The Root Mean Square Error of the crest position for C1 and C2 are respectively $RMSE_{C1}$ = 9.35 m and $RMSE_{C2}$ = 2.89 m. On this transect, all dune crests have moved of about 20 m toward the east. This short movement combined with the low dune height explains the good BSS on both configurations. However, by comparing the RMSE on the crests positions, configurations C1 is accurate on the heights estimation but not on the crests positionning and therefore on the migration process. This is consistent with the results reported by Krabbendam et al. (2021) who have shown that the BSS should be considered carefully based on the results on 2D modelling along dunes.

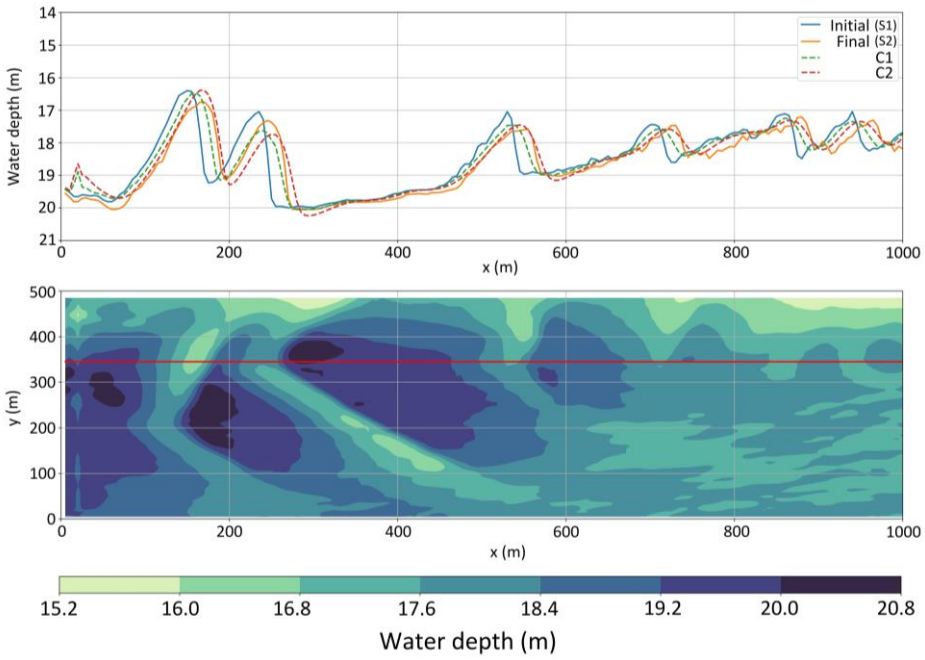

Figure 7. (top) Longitudinal profiles of the initial (S1) and final (S2) observations compared with C1 and C2 configurations results. (bottom) Synoptic view of the bathymetry estimated by C2 configuration. The red line represents the location of the transect.

The validation using a single longitudinal profile and the comparison of crest position show that the C2 configuration performs better than C1 configuration. However, because of the presence of barchans and sinuous dunes, the comparison depends on the transect location. Following the same procedure, the bathymetric profile is extracted along a line perpendicular to the crest line of D2 crossing the area from South-East to North-West (Figure 8). Here the profile also catches the

third dune. Contrary to the previously analysed profile, both configurations do not model correctly the dynamic of dune D2. Difference between S1 and S2 shows that D2 migrates toward the east but experienced a large decrease of its crest height, which is not reproduced by the model. Here the crest height drop by about 0.7 m while C1 and C2 estimates an increase of respectively 0.1 and 0.3 m. Following these profiles, the estimations are not classified as excellent with BSS lower than 0.5 (BSS_{C1} = 0.38 and BSS_{C2} = 0.45). The RMSE should not be applied on only two crests positions. Therefore model and observation are only compared by the difference in meters. For both configurations, the position of D2 crest is well represented with a difference of 5 m only. However for D3, both C1 and C2 do not catch the strong movement occuring during the study period with respectively a difference of 15 and 10 m. By considering only the D2 dune, and this transect, the best model configuration is C1, which contradicts previous results.

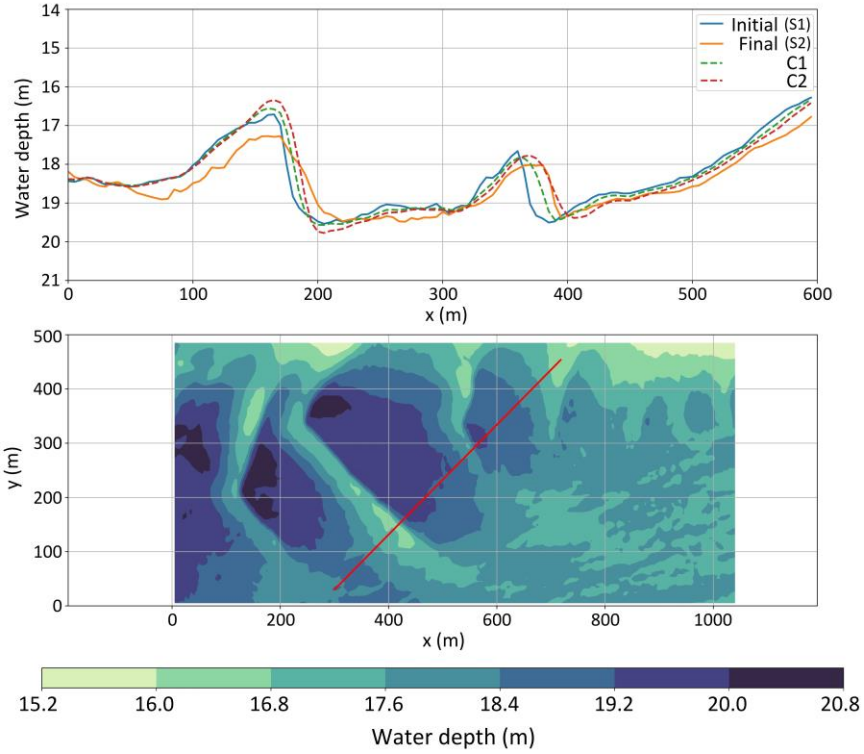

Figure 8. (top) Bathymetric transect of the initial and final observations compared with C1 and C2 configurations results extracted along a line perpendicular to D2 crest line. (bottom) Synoptic view of the bathymetry estimated by C2 configuration. The red line represents the location of the transect.

3.3 Comparison with observations over the area

To the authors knowledge, no validation was performed with a three-dimensional modelling of marine dunes against an observed bathymetry. Therefore, the validation process in this section is based on a classical procedure used to validate morphodynamic modelling of sand banks or coastlines (Sutherland et al., 2004 ; Ruggiero et al., 2009 ; Ranasinghe et al., 2011 ; Luijendijk et al., 2016). Following it, the BSS is estimated for both configurations considering the entire B1

domain. Results show that C2 better represents the dune migration with a BSS_{C2} = 0.73 compared to C1 with a BSS_{C1} = 0.56. Here the BSS over the whole domain is lower than the BSS calculated using the longitudinal profile as it considers the error spotted on the southern part of D2 dune. Both configurations could however be considered as excellent which could be enough to validate the model. To identify the source of the error of both configurations, the Murphy-Epstein decomposition is applied and the results reported in the following Table 2. For both configurations the average bed level error γ and the normalization term ε are similar with a value of 0.04. Bottom roughness does not induce significant influence of these terms consistently with the results reported by Sutherland et al. (2004). A slight difference is estimated for the amplitude error with 0.07 for C1 and 0.002 for C2. These values are still close to zero which indicates an almost perfect modelling of the transported volume. The main source of error here comes from the phase (i.e. the position of the dunes), with α_{C1} = 0.65 and α_{C2} = 0.75.

Variable name	α	β	γ	ε
C1	0.65	0.07	0.04	0.04
C2	0.75	0.002	0.04	0.04

Table 2. Murphy-Epstein decomposition of the Brier Skill Score estimated for both C1 and C2 configuration over the entire B1 area.

To analyse this error, longitudinal transects are extracted every 5 m (the model resolution) and an average migration is estimated considering only the movement of the crests. All crests move as expected toward the east with average displacements ranging from 18.75 m for D5 to a maximum of 23.13 m for D4. The RMSE of crest positions are estimated for each dune independantly (Table 3). As a reminder, consistently with the model, observations were projected on a 5 m resolution grid. Therefore, the RMSE lower than 5 m calculated for C2 over dunes D1, D3, D4 and D6 and equal to 5 m for D5 clearly demonstrate that C2 configuration results can be considered as excellent. However, in the case of C1 configuration, bottom roughness is too low for the model to estimate a sufficient migration during the period. This lead to high difference of around 10 m for all dunes. Compared to the observed displacement of about 20 m of each dune, this can be considered as a strong error and cannot be considered as a reliable comparison. This is in line with the previously described results which shows that C1 configuration is not acceptable in term of crest positions. Both configurations show however strong RMSE for D2, with 16.6 and 14 m for C1 and C2, respectively. For C1 this demonstrates that the representation on all dunes have a lack of precision while it shows, for C2, a lack of precision on one dune only.

Table 3. Mean migrations and Root Mean Square Error (RMSE) of the crests position for each dune for both C1 and C2 configurations.

Dune name	D1	D2	D3	D4	D5	D6
Mean migration (in m)	19.17	20.93	20.7	23.13	18.75	22.11
RMSE C1	10.38	16.6	11.51	12.78	10.75	11.81
RMSE C2	5.31	14	4.38	3.19	5	2.56

Here the results show that the use of the BSS over the whole area does not seem adapted for this kind of modelling. The validation process needs to be improved with an analysis of each dune position. However, in the current case, the combined BSS with the analysis of the crest position is easy to perform because of the small number of dunes but, in the case of the presence of dozens of dunes, this analysis is too labourious to be used. This procedure should then be improved in order to evaluate the height and crest positions in a reliable way.

3.4 Three-dimensional validation

In this section, a validation method of a three-dimensional dune migration modelling is proposed. It is based on two main dimensions. The vertical dimension with the estimation of the depths and dune heights and the horizontal dimension with the position of the crests and troughs of each dune.

Vertical validation

As described earlier, the vertical validation over an area is made by the calculation of the Brier Skill Score (BSS) which considers the entire B1 domain. However, contrary to the modelling of a sand bank or a coastline, here the focus is made on the modelling of marine dunes which represent only a small part of the actual domain. In fact, another particularity of the B1 domain, is that it is composed by large plain areas where only secondary dunes are present. The model does not consider these shapes, as they are below the resolution required and not the focus of the present study, and smoothed the bathymetry leading to a global error. Including these plain areas in the validation process means that the dune migration validation depends on the correct modelling of areas that are not related to the very large dunes. To overcome this issue, it is necessary to consider only the dune areas. This requires to accurately identify both crests and troughs. In the preliminary analysis (Nexer et al, 2023), the crests were considered as the local minima of water depths. Consistently, the troughs were identified as the local maxima of water depths. However, in the marine environment, through identification is complex and they are either considered as the foot of the stoss or lee slope (Duffy, 2012) or the point where the maximum value of the curvature is estimated (Van Dijk et al., 2012; Lebrec et al., 2022). Duffy (2012) considers using the foot of the stoss or lee slope for a solitary bedform while here multiple dunes are present. The definition based on the calculation of the curvature seems then to be adapted for the current case and the methodology described by Lebrec et al. (2022) is applied over the B1 domain.

All longitudinal profiles were extracted every 5 m along the y-axis for both observations and model results. Despite the low-pass filter, some remaining secondary bedforms could induce multiple crests detection. The point with the minimum water depth is then considered as the crests of each dunes. The curvature is calculated as the second derivative of the bathymetric profile. The first local maximum of curvature on each side of the crests positions is considered as the eastern and western troughs of the dune.

Considering the eastern migration pattern, the area occupied by each dunes is taken as starting on the west with the western trough of the initial observation and, on the east, with the eastern trough of the final observation. The 6 dunes areas are then identified as shown on Figure 9. To avoid any boundary issues, the model and observations data do not account for the first 50 m along to the boundaries. This limits the identification of the western trough of D1 which will not be accounted into the comparison process. The identified areas show that dunes D1 and D2

follow each other on their northern part while there is a large plain area that separates them on the southern part. The same thing is observed for D5 which northern part sticks with the southern part of D6. The other dunes D3 and D4 are isolated with plain areas that separates them from the others.

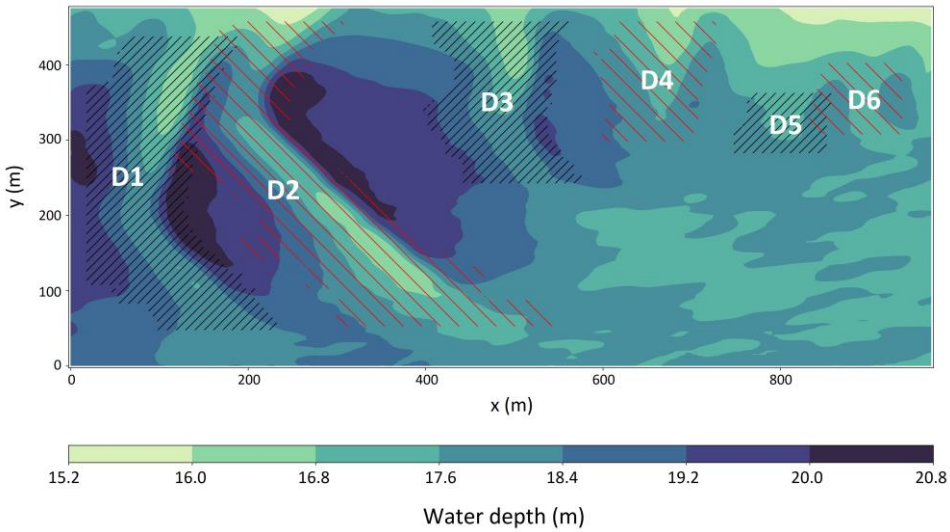

Figure 9. Area of the six dunes over the B1 domain. The colormap represents the bathymetry estimated by configuration C2.

Using this identification, the Brier Skill Score is applied on the six areas for both configurations. This allows to assess the capability of the model to simulate the area where there is a dune movement. As described earlier, it also discards the large plain on the south-east, which represents almost 1/4th of the model domain, and also other part which are not related to the dunes. For C1 and C2 the BSS is respectively of 0.62 and 0.81. Here the difference with the BSS estimated by considering the entire B1 area (BSS_{C1} = 0.56 ; BSS_{C2} = 0.73) shows that C2 was slightly more penalized by the plain areas in the estimation of its accuracy. This could be explained by the fact that C2 has less error over the dune than C1. The error on the plains areas on the south-east could then become more important in the entire calculation which would then reduce the skill score.

The BSS can also be applied over each dune separately. The results show that for both configurations, D2 is the least well represented with a BSS_{C1-D2} = 0.51 and BSS_{C2-D2} = 0.68 (Table 4). The scores for C1 configuration are quite similar for all the other dunes except D1 while for C2 there are larger differences between D2 and all other dune that show BSS ≥ 0.8. It highligths the fact that the model does not catch all changes in D2.

Table 4. Brier Skill Score (BSS) estimated for each dune areas for C1 and C2 configurations.

Dune name	D1	D2	D3	D4	D5	D6
C1	0.74	0.51	0.68	0.62	0.62	0.52
C2	0.9	0.68	0.92	0.88	0.83	0.8

Horizontal validation

The crest and trough positions are compared for both configurations with the new identification methodology. The RMSE of the crest and trough positions is estimated for all dunes together except for the western trough for which the dune D1 is not considered as its location is limited by the area boundaries. These results first highlight strong differences of the trough locations with the observations for both configurations. The western troughs are the least well represented for C1 and C2 with RMSE of respectively 21.84 and 17.89 m while on the eastern troughs the RMSE is better with respectively 17.74 and 12.84 m. This highligths that even using the identification process described by Lebrec et al. (2022), the location of the troughs in a marine environment cannot be accurate enough for this kind of comparison. For long term simulations like the present study, the crests positions seems then to be the better choice for the migration validation.

Table 5. Root Mean Square Error (RMSE) estimated for western and eastern troughs and crest positions for both C1 and C2 configurations.

Variable name	Western troughs	Crests	Eastern troughs
C1	21.84	13.1	17.74
C2	17.89	8.57	12.84

In the present study, the crest locations RMSE demonstrate the difference between configurations with for C1 and C2 values of respectively 13.1 m and 8.57 m. The error estimated with C2 configuration is not far fom the model resolution (5 m) but cannot be considered as excellent. Following the mathematical definition of the Root Mean Square Error, this statistics would give more weight to the strong errors. This means that if the crest position is not accurately modelled on a small part of the dune, this would increase the RMSE. Figure 10 shows the crest locations for initial and final observations and for C1 and C2 configurations. It highlights that globally the crests position estimated by C2 configuration is close to the reference while C1 estimations are almost entirely “half way” between initial and final observations. In the case of C2, the crests positions even overlapped with the reference on the major part of D3, D4 and D6. However, the crest position during the second bathymetric survey shows that the D2 has moved from its initial position by about 40 m on its southern horn. Both configurations did not represent this movement and the RMSE is then naturally increased by it. A second limitation of the RMSE here, is also that it does not consider the crests initial position and it could be difficult to assess the precision of a model.

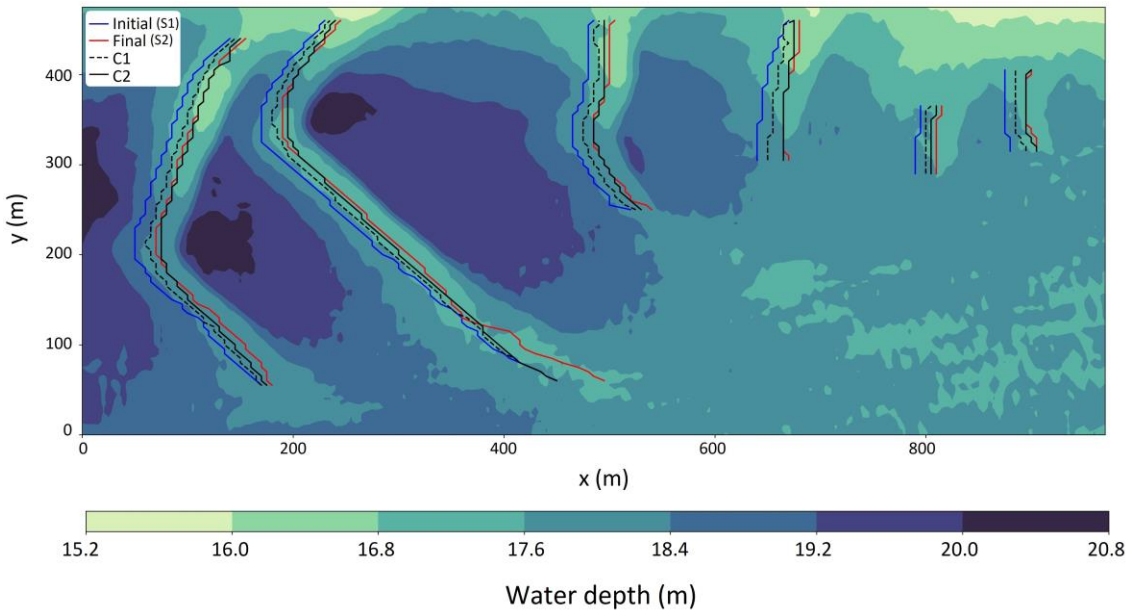

Figure 10. Locations of dunes' crests of initial and final observations compared with predictions of C1 and C2 configurations. The colormap represent the bathymetry estimated by C2 configuration.

Sutherland et al. (2004) have described that a statistic should be transferable from a dataset to another. Therefore, the use of the Brier Skill Score might be a good option to include the initial crest positions and allow to estimate the model accuracy. The proposition made here is then to estimate the BSS by considering all positions of crests as the dataset. For both C1 and C2 the estimated value is respectively BSS_{C1} = 0.62 and BSS_{C2} = 0.84. Here the difference estimated between the configurations is of the same order as the difference estimated for the vertical comparison. However, the classification proposed by Sutherland et al. (2004) might not be adapted here and these scores should not be considered the same way. Indeed, as described before, C1 crest position is almost entirely "half way" between initial and final observations. The score of 0.62 is thus logical. An "excellent" modelling of the crests position should so be considered for scores greater or equal to 0.8 which, as described by C2 configuration results, induce an accurate representation of the crests positions.

Using this methodology, both vertical and horizontal dimension show a good skill score for the C2 configuration. On the contrary, C1 is accurate on the vertical dimension but does not represent well the crests' positions. The C2 configuration is therefore considered as valid here while C1 is not.

4. Discussion

4.1 Two and three dimensions

Among the different morphodynamic studies, most of them use a two-dimensional vertical model (2DV) (Nemeth et al., 2007 ; Tonnon et al., 2007 ; Krabbendam et al., 2021). In these studies, the dune field is composed by rectilinear dunes. The use of a 2D validation process

based on transect comparison is so well fitted. This is however not the case for some 3D morphodynamic models. Indeed, as shown by the results of the 2D analysis, the barchan dune D2 has a faster crest displacement on its toe in the north than on its horn in the south (nomenclature based on Couldrey et al., 2019). This is in line with the results of Charru and Laval (2013), who have reported a reduction of the current intensity over the horns of a barchan. The model is so able to reproduce this migration on its northern part but fails on its southern part with almost no displacement of the crest (Figures 7 and 8). This demonstrates the need to prioritize a validation over the area or at least over multiple transects to avoid missing such errors that could occurs over small areas.

The 3D validation method also has the advantage to better assess the difference between configurations. Over the first transect (Figure 7), the difference between C1 and C2 BSS is 0.12 (BSS_{C1} = 0.75 ; BSS_{C2} = 0.87) while over the second transect it is equal to 0.07 (BSS_{C1} = 0.38 ; BSS_{C2} = 0.45). Both configurations could then be considered equivalent in term of validity. On the contrary, the difference between the skill scores considering the B1 area is 0.17 (BSS_{C1} = 0.56 ; BSS_{C2} = 0.73). A value that is even increased to 0.19 when considering the dunes' areas (BSS_{C1} = 0.62 ; BSS_{C2} = 0.81). Therefore, a 3D comparison accentuates the differences between the configurations and allows a better assessment of numerical modelling results. A 3D validation process might then need to be considered on an area even if the dunes are rectilinear. This could bring more insight about the configurations reliability than a 2D analysis and improve the validation process itself.

4.2 Limitations and advantages of the proposed method

The previous results demonstrate that the use of a 3D model with a 3D validation method is necessary in the current case. However, regarding the vertical dimension, the method used for coastlines or sand banks does not seems adapted to marine dune migration modelling. By considering the entire domain for the BSS calculation, the large plains in the southeastern part of the domain would be included. This implies that the validation of the dunes' migration modelling depends on the correct modelling of secondary bedforms located hundreds of meters away from the primary dunes. Here, the model does not consider these bedforms and smooths the entire southeastern area of the B1 domain. This leads to a source of error which reduces the BSS. The proposed method considers to avoid these plains to focus on the areas where the dunes migrate. The identification of these areas is however a limitation of the method. The comparison made on the trough and crest positions shows strong errors on the trough positions compared to the crests. This error could be attributed to a difficult identification of the troughs. Indeed, as described by Lefebvre et al. (2021), in an environment dominated by tidal current, bedforms have steeper slopes close to the crest, and flat troughs. This is confirmed here by the filtered profiles shown on Figure 11. The slope is calculated on the same longitudinal profile displayed on Figure 7 for the initial observation. The maximum angle is found on the upper part of the lee side, closer to the crest than to the eastern trough with angles reaching a maximum of 14° for D2. Regarding the horizontal position, the maximum slope of dune D4 is also closer to the crest while for the others it is located on the middle part of the lee side. This facilitates the identification of the crests but it is quite difficult to identify the troughs. The dune areas identified here using the methodology defined by Lebrec et al. (2022) is limited as their boundaries are defined by the western and eastern troughs. Moreover, this also induce that the method should be adapted to the environment. In the marine environment, the crests positions are easily identified and then the comparison of their position with the observations make sense. In rivers however, Cisneros et al

(2020) have reported that dunes have a relatively flat crest and maximum slope over their lower lee side. The method might need to be applied on the troughs positions in the river environment to consider this difference.

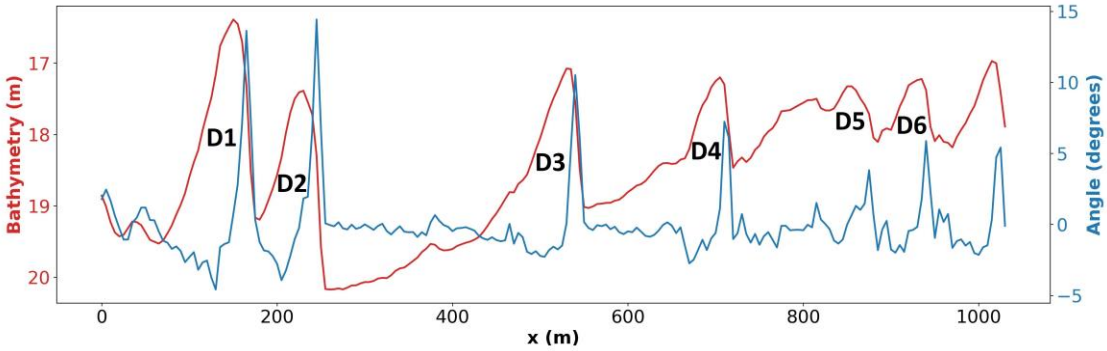

Figure 11. (Red) Longitudinal profiles of the initial observations extracted along the transect represented on Figure 7. (Blue) Slope on the bathymetry. The calculation is based on the bathymetric profile represented by the blue line.

The comparison of the crest (or trough) position is mostly performed using the RMSE in 2DV models. However, in a three-dimensional validation that considers all crests positions, this leads to two issues that should be considered. First, in the present study, the major source of error on both configurations comes from the southern part of dune D2. Observations show a large displacement of the crests of about 30-40 m while both configurations do not estimate any movement. This explain the RMSE that is high even for C2 (Table 2) which is considered as valid. However, when it comes to the modelling of the morphodynamic of an area, even for a sand bank or other cases, the validation process should focus on knowing if the model is globally accurate. Here if the RMSE is applied on all crest positions, it would be increased by this error occuring on a small part of one dune. The entire simulation would then be penalized. Other metrics could have been used such as the Mean Average Error (MAE) or the Mean Square Error (MSE), however same as the RMSE all these metrics do not account for the initial crest position. This lead then to the second issue, which is that the modelling it made to represent the migration of the dune and not the crest positions. Using the BSS puts the error in context. This leads however to another limitation of the proposed method. All dunes migrate following the eastern direction. Here it allows an easy comparison of the crest positions with only a difference in the longitudinal direction. However, over a larger domain, multiple dune migration direction could be present. The method should then be adapted to the domain by comparing the dune migration in the correct direction.

5 Conclusions

In the context of the numerical modelling of a dune field, the question of the validation of a three-dimensional model was addressed. This was studied with validation methods based on the comparison with bathymetric survey using either a transect or the entire area to assess the model reliability. The main outcomes of the study are as follows :

1. The application of the Brier Skill Score on the entire domain does not seem to be adapted to validate a morphodynamic model focusing on marine dune migration. In this case the southeastern part of the domain is composed by a large plain area which is unrelevant to assess the model reliability. The method proposed here is then to only consider the dunes' areas to estimate this score and avoid considering unrelevant areas in the validation process.

2. In the same context, the calculation of the RMSE of the crest positions does not seem to be adapted here to the validation process. This score will be boosted by a strong difference occuring on a small part of a dune. Therefore, to overcome this issue, the proposed method considers the application of the Brier Skill Score by considering the crest positions as the dataset. The error is then put in context and allows to better assess the model capability.

The findings of this study do not have the intention to question the validity of other models and more studies using this method needs to be performed to assess its reliability. The modelling of a marine dune field is quite new and the method that is described here is then a proposal to see the validation of this kind of model in another way.

Acknowledgments

This work is part of the MODULLES project which receives funding from France Energies Marines and its members and partners, as well as French State funding managed by the French National Research Agency under the France 2030 Investment Plan (ANR-10-IEED-0006-34).

References

Auclair, F., Benshila, R., Bordois, L., Boutet, M., Brémond, M., Caillaud, M., Cambon, G., Capet, X., Debreu, L., Ducousso, N., Dufois, F., Dumas, F., Ethé, C., Gula, J., Hourdin, C., Illig, S., Jullien, S., Le Corre, M., Le Gac, S., et al. (2022), Coastal and Regional Ocean COmmunity model (1.3). https://doi.org/10.5281/zenodo.7415343

Barrie, J.V., Conway, K.W. (2014), Seabed characterization for the development of marine renewable energy on the Pacific margin of Canada. *Continental Shelf Research*, *83*, 45-52. https://doi.org/10.1016/j.csr.2013.10.016

Belderson, R.H., Johnson, M.A., Kenyon, N.H. (1982), Bedforms. *Offshore Tidal Sands, Processes and Deposits*, Chapman and Hall. https://doi.org/10.1007/978-94-009-5726-8.

Bennet, W.G., Karunarathna, H., Reeve, D.E., Mori, N. (2019), Computational modelling of morphodynamic response of a macro-tidal beach to future climate variabilities. *Marine Geology*, 415. https://doi.org/10.1016/j.margeo.2019.105960.

Blaas, M., Dong, C., Marchesiello, P., McWilliams, J.C., Stolzenbach, K.D. (2007), Sediment-transport modeling on southern californian shelves: A ROMS case study. *Continental shelf research, 27*, 832-853. https://doi.org/10.1016/j.csr.2006.12.003.

Blondeaux, P., Vittori, G. (2016), A model to predict the migration of sand waves in shallow tidal seas. *Continental Shalef Research, 112*, 31-45. https://doi.org/10.1016/j.csr.2015.11.011.

Bonnefille, R., Lepetit, J.-P., , Graff, M., Leroy, J. (1971), Nouvel avant-port de Dunkerque, Mesure en nature. *Laboratoire National d'Hydraulique, Report HC042/05*.

Charru, F., Laval, V. (2013), Sand transport over a barchan dune. *MARID IV – 15 & 16 April 2013- Bruges, Belgium*.

Cisneros, J., Best, J., van Dijk, T., Paes de Almeida, R., Amsler, M., Boldt, J., Freitas, B., Galeazzi, C., Huizinga, R., Ianniruberto, M., Ma, H., Nittrouer, J.A., Oberg, K., Orfeo, O., Parsons, D., Szupiany, R., Wang, P., Zhang, Y. (2020), Dunes in the world's big rivers are characterized by low-angle lee-side slopes and a complex shape. *Nature Geoscience, 13*, 156-162. DOI : 10.1038/s41561-019-0511-7.

Couldrey, A., Knaapen, M., Marten, K., Whitehouse, R. (2019), Barchan vs Monopile : what happens when a barchan dune finds an obstacle in its path ?. *Marine and River Dune Dynamics – MARID VI*, 1-3 April 2019, Bremer, Germany.

Dam, G., van der Wegen, M., Labeur, R.J., Roelvink, D. (2016), Modeling centuries of estuarine morphodynamics in the Western Scheldt estuary. *Geophysical Research Letters, 43*, 3839-3847. doi:10.1002/2015GL066725.

Damen, J.M., van Dijk, T.A.G.P., Hulscher, S.J.M.H. (2018), Spatially varying environmental properties controlling observed sand wave morphology. *Journal of Geophysical Research: Earth Surface*, 123(2), 262-280. doi:10.1002/2017JF004322

van Dijk, T.A.G.P., van Dalfsen, J.A., Van Lancker, V., van Overmeeren, R.A., van Heteren, S., Doornenbal, P.J. (2012), Benthic Habitat Variations over Tidal Ridges, North Sea, the Netherlands. *Seafloor Geomorphology as Benthic Habitat*, 241–249. https://doi.org/10.1016/B978-0-12-385140-6.00013-X

Doré, A., Bonneton, P., Marieu, V., Garlan, T. (2018), Observation and numerical modeling of tidal dune dynamics. *Ocean dynamics, 68*, 589-602. https://doi.org/10.1007//s10236-018-1141-0.

Duffy, G. (2012), Patterns of morphometric parameters in a large bedform field: Developpement and application of a tool for automated bedform morphometry. *Irish Journal of Earth Sciences, 30*, 31-39. doi.10.3318/IJES.2012.30.31.

Ernsten, V.B., Noormets, R., Winter, C., Bartholomä, A., Flemming, B.W., Bartholdy, J. (2004), Development of subaqueous barchan dunes due to lateral grain size variability. *MARID, Enschede Netherlands*, p.8.

Knaapen, M.A.F., Hulscher, S.J.M.H., Vriend, H.J., Stolk, A. (2001), A new type of sea bed waves. *Geophysical Research Letters, 28*, 1323-1326. https://doi.org/10.1029/2000GL012007.

Krabbendam, J., Nnafie, A., de Swart, H., Borsje, B., Perk, L. (2021), Modelling the past and future evolution of tidal sand waves. *Journal of marine science and engineering*, *9*, 1071. https://doi.org/10.3390/jmse9101071.

Le Bot, S., Trentesaux, A. (2004), Types of internal structure and external morphology of submarine dunes under the influence of tide- and wind-driven processes (Dover Strait, northern France). *Marine Geology*, *211*, 143-168. https://doi.org/10.1016/j.margeo.2004.07.002.

Lebrec, U., Riera, R., Paumard, V., O'Leary, M.J., Lang, S.C. (2022), Automatic Mapping and Characterisation of Linear Depositional Bedforms: Theory and Application Using Bathymetry from the NorthWest Shelf of Australia. *Remote Sensing*, *14*, 280. DOI : 10.3390/rs14020280.

Lefebvre, A., Herrling, G., Becker, M., Zorndt, A., Krämer, K., Winter, C. (2021), Morphology of estuarine bedforms, Weser Estuary, Germany. *Earth Surface Processes and Landforms*, 1-15. https://doi.org/10.1002/esp.5243.

Luijendijk, A.P., Ranasinghe, R., de Schipper, M.A., Huisman, B.A., Swinkels, C.M., Walstra, D.J.R., Stive, J.F. (2017), The initial morphological response of the Sand Engine: A process-based modelling study. *Coastal engineering*, *119*, 1-14. http://dx.doi.org/10.1016/j.coastaleng.2016.09.005.

Németh, A.A., Hulschher, S.J.M.H., Van Damme, R.M.J. (2007), Modelling offshore sand wave evolution. *Continental Shelf Research, 29*, 713-728. https://doi.org/10.1016/j.csr.2006.11.010.

Nexer, M., Bacha, M., Bary, M., Gangloff, A., Robert, A., Amara, R., Blanpain, O., Parent, B., Desroy, N., Garlan, T., Le Bot, S., Michelet, N., Quillien, N. (2023), Les dunes sous-marines et leur écosystème sous contraintes anthropiques. Recommendation report of the DUNES project, France Energies Marines.

Ranasinghe, R., Swinkels, C.M., Luijendjik, A.P., Roelvink, J.A., Bosboom, J., Stive, M.J.F., Walstra, D.J.R. (2011), Morphodynamic upscaling with the MORPHAC approach: dependencies and sensitivities. Coastal Engineering, *58*. https://doi.org/10.1016/j.coastaleng.2011.03.010

Ruggiero, P., Walstra, D.J.R., Gelfenbaum, G., Van Ormondt, M. (2009), Seasonal-scale nearshore morphological evolution: Field observations and numerical modeling. *Coastal Engineering*, *56*, 1153-1172. doi:10.1016/j.coastaleng.2009.08.003.

Sutherland, J., Peet, A.H., Soulsby, R.L. (2004), Evaluating the performance of morphological models. *Coastal engineering*, *51*, 917-939. https://doi.org/10.1016/j.coastaleng.2004.07.015.

Scott, T.R., Mason, D.C. (2007), Data assimilation for a coastal area morphodynamic model: Morecambe Bay. *Coastal engineering*, *54*, 91-109. https://doi.org/10.1016/j.coastaleng.2006.08.008.

Tonnon, P.K., van Rijn, L.C., Walstra, D.J.R. (2007), The morphodynamic modelling of tidal sand waves on the shoreface. *Coasta*l engineering, *54*, 279-296. https://doi.org/10.1016/j.coastaleng.2006.08.005.

Van den Berg, J., Sterlini, F., Hulscher, S.J.M.H., van Damme, R. (2012), Non-linear process based modelling of offshore sand waves. *Continental shelf research*, *37*, 26-35. https://doi.org/10.1016/j.csr.2012.01.012.

Warner, J. C., Sherwood, C. R., Signell, R. P., Harris, C. K., and Arango, H. G. (2008), Development of a three-dimensional, regional, coupled wave, current, and sediment-transport model. *Computers & Geosciences*, *34*(10), 1284–1306. https://doi.org/10.1016/j.cageo.2008.02.012.

Whitehouse, R.J.S., Damgaard, J.S., Langhorne, N. (2000), Sandwaves and seabed engineering: the application to submarine cables. *Proceeding of Marine Sandwaves Dynamics*, MARID, 227-234.

Willmott, C. (1981), On the validation of models. *Phys. Geogr*., *2*, 184–194. https://doi.org/10.1080/02723646.1981.10642213

Wu, W., Lin, Q. (2014), Nonuniform sediment transport under non-breaking waves and currents. *Coastal Engineering*, *90*, 1-11. http://dx.doi.org/10.1016/j.coastaleng.2014.04.006.